



# Suppression of edge cracking in layered ceramic composites by edge coating

Adam J. Monkowski, Glenn E. Beltz \*

*Department of Mechanical Engineering, University of California, Santa Barbara, CA 93106-5070, USA*

Received 29 April 2004; received in revised form 14 June 2004  
Available online 25 August 2004

---

## Abstract

A strategy is proposed to reduce surface tensile stresses that develop in ceramic microlaminate structures. As a specific example, surface stresses, which can lead to unwanted edge cracking, appear within a thin alumina/mullite layer bounded by thicker alumina layers after fabrication at some elevated temperature and subsequent cooling. A stress analysis is performed using the finite element method on a geometry in which the (edge) surface of the ceramic sandwich structure has been coated with an overlayer of the alumina/mullite material with thickness proportional to the initial buried layer thickness. These analyses show there is a critical thickness of the overlayer at which the surface tensile stresses can be reduced to zero. Stress concentration factors are calculated numerically for cracks propagating through this structure, and thus the resistance to surface cracking is quantified.

© 2004 Elsevier Ltd. All rights reserved.

---

## 1. Introduction

The major drawback of ceramics as structural materials is their brittleness. Brittle materials contain an unknown variety of cracks and flaws that are inadvertently introduced during processing and surface machining (Lange, 1989; Lawn, 1993; Ho et al., 1995; Hillman et al., 1996; Oechsner et al., 1996; Green, 1998; Rao et al., 1999). As ceramics are increasingly being deployed in structural applications, a large research effort has been devoted to the exploration of methods to increase their toughness and to inhibit crack propagation. One such method centers around using layered ceramic structures that exhibit high fracture toughness for cracks propagating perpendicular to their layers (Hillman et al., 1996; Oechsner et al., 1996; Rao et al., 1999; McMeeking and Hbaieb, 1999; Hbaieb and McMeeking, 2002; Jónsdóttir et al., in press).

---

\* Corresponding author. Tel.: +1 805 8933354; fax: +1 805 8938651.  
E-mail address: [beltz@engineering.ucsb.edu](mailto:beltz@engineering.ucsb.edu) (G.E. Beltz).

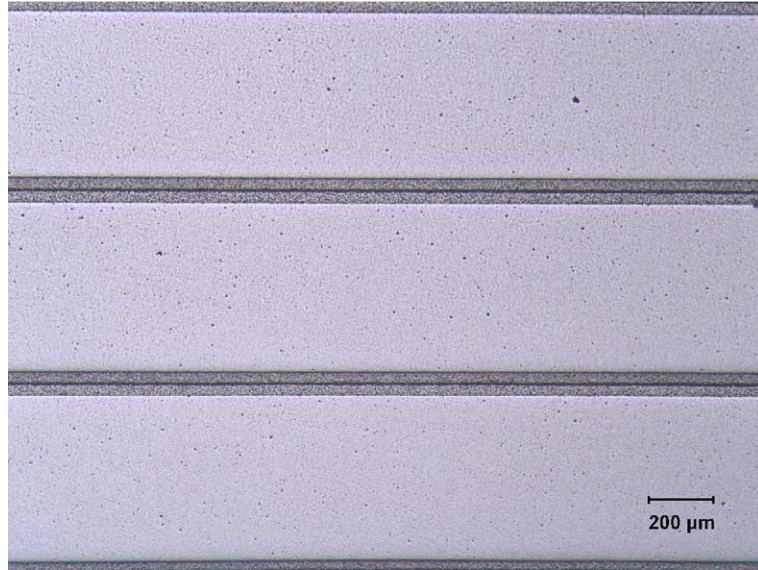


Fig. 1. Edge view of an alumina-based laminate structure, in which edge cracks have initiated at the surface and propagated inward. The thin layers consist of 50% alumina and 50% mullite (by volume), and the thick layers consist of 95% alumina and 5% zirconia. The thickness of the compressive layer is 50  $\mu\text{m}$ . The average crack penetration is estimated as 75  $\mu\text{m}$  (photograph courtesy of H. Moon).

In particular, Lange (2003) and coworkers (Rao et al., 1999; Fair, 2003; Snyder, 2004) are exploring a class of powder-processed ceramic composites that use very thin compressive layers consisting of an alumina ( $\text{Al}_2\text{O}_3$ )/mullite<sup>1</sup> mixture to arrest incipient cracks. However, cracks that initiate on the surface of these structures and propagate *parallel* to the layers can grow in the absence of any toughening mechanism to inhibit their advancement (see Fig. 1). As the study of layered ceramic structures has progressed, some focus has been given to the residual stresses in structures that cause the development of these undesirable surface cracks (Ho et al., 1995).

When a layered structure of two materials with different coefficients of thermal expansion ( $\alpha_1 \neq \alpha_2$ ) is fabricated at a high temperature,  $T_0$ , and cooled to a lower temperature,  $T$ , a mismatch strain of

$$\varepsilon_m = \int_T^{T_0} (\alpha_2 - \alpha_1) dT \quad (1)$$

develops. Let us assume  $\alpha_2 > \alpha_1$ , such that  $\varepsilon_m$  is positive. Far from external boundaries, the residual stresses resulting from this mismatch strain are biaxial and compressive in nature; however, on and near the surface, in the layer with smaller coefficient of thermal expansion, the residual stress is *tensile* in nature normal to the centerline of the layer. Consider a laminate, which is balanced (so that no bending takes place) with layer thicknesses  $t_1$  and  $t_2$ . Examining the case where one layer is much thicker than the other ( $t_1/t_2 \rightarrow 0$ ) and, assuming no elastic modulus mismatch, the biaxial stress in the thin layer (#1) *far* from the surface can be expressed as

$$\sigma_{xx}^{(1)} = \sigma_{zz}^{(1)} = -\sigma_m = -E_1 \varepsilon_m (1 - \nu_1)^{-1}; \quad \sigma_{yy}^{(1)} = 0 \quad (2)$$

<sup>1</sup> Mullite is an inexpensive ceramic with nominal composition  $3\text{Al}_2\text{O}_3\text{-}2\text{SiO}_2$ .

where  $E_1 = E_2 = E$  is Young’s modulus and  $\nu_1 = \nu_2 = \nu$  is Poisson’s ratio. For more general situations, accounting for modulus mismatch and layers of comparable thicknesses, the relevant expression can be found in published work by Ho et al. (1995), Hillman et al. (1996), Oechsner et al. (1996), and Rao et al. (1999).

Near the boundaries where the layers terminate (see Fig. 2), the situation is somewhat different. An analytical solution to the stress field near the surface can be found from a superposition scheme described by Ho et al. (1995), wherein the residual stress problem for this structure can be represented as the sum of Problem A and Problem B as shown in Fig. 2. In Problem A, the two thick layers are stress-free, and the thin layer is under biaxial compression of magnitude  $\sigma_m$  in the plane of the layer. A traction of magnitude  $\sigma_m$  (perpendicular to the surface) is applied to layer 1, keeping the stress distribution within layer 1 uniform. Problem B consists of the identical geometry, but with a tensile traction of magnitude  $\sigma_m$  applied where layer 1 intersects the surface. The superposition of these two problems gives the residual stress problem initially envisioned, that is, one having a traction-free boundary condition at the surface and the proper misfit stress field for large  $x$ . Integrating the solution for a point force on a free surface over the region where the tractions are applied can be used to solve Problem B. Performing this integration and superposing with the solution for Problem A yields the results

$$\sigma_{xx} = \frac{\sigma_m}{2\pi} [2(\theta_1 - \theta_2) - (\sin 2\theta_1 - \sin 2\theta_2)] - \sigma_m \tag{3a}$$

$$\sigma_{yy} = \frac{\sigma_m}{2\pi} [2(\theta_1 - \theta_2) - (\sin 2\theta_1 - \sin 2\theta_2)] \tag{3b}$$

$$\sigma_{xy} = \frac{\sigma_m}{2\pi} [\cos 2\theta_2 - \cos 2\theta_1] \tag{3c}$$

for the stress field in the thin layer. The angles  $\theta_1$  and  $\theta_2$  correspond to those labeled in Fig. 3. A key stress component in question is  $\sigma_{yy}$ , because this is what would drive any incipient crack that nucleates at the surface and propagates along the  $x$ -direction. Fig. 3 shows  $\sigma_{yy}$  for several locations within the structure. This graph shows that along the entire surface of layer 1, there is a residual *tensile* stress equal to  $\sigma_m$ , which decays with distance into the structure.

Even though the thin layer has been engineered to be in nominal *compression*, the tensile stress on the surface can lead to the nucleation and propagation of cracks into the structure. The mechanics of this edge phenomenon have been discussed in detail by Ho et al. (1995), where design rules were derived for minimizing the likelihood of fracture in such structures.

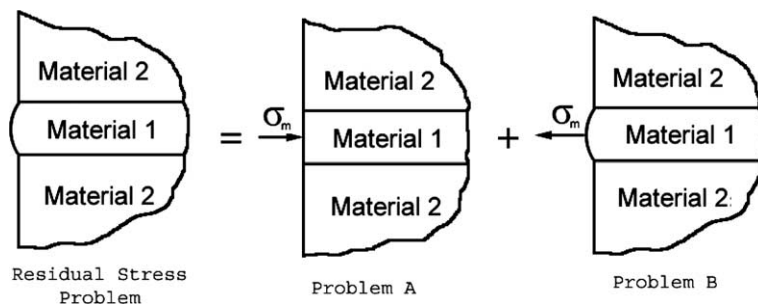


Fig. 2. The stresses near the edge of a sandwiched thin film can be obtained from the superposition of two other problems: (A) involves a pressure distribution of magnitude  $\sigma_m$  in addition to the thermal mismatch; and (B) consists of a tensile traction of magnitude  $\sigma_m$  with no additional thermal mismatch.

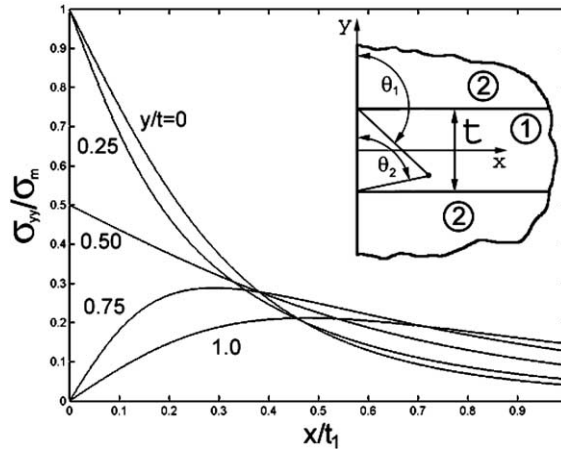


Fig. 3. Distribution of stress near the edge of a layered composite, from analytical solution (Eq. 3b). The elastic mismatch in this system is assumed to be zero.

While layered structures are resistant to crack growth in directions that impinge on interfaces, they are not ideal for resisting crack growth in directions parallel to interfaces. The development of novel three-dimensional architectures is underway (e.g., cylindrical shells or spherical shells of compressive material) to address this problem (Jónsdóttir et al., *in press*; Fair, 2003; Snyder, 2004). However, these complex structures are still susceptible to edge cracking wherever the interfaces abut a free surface. A method for eliminating the residual tensile stresses at the surface in conventional layered structures (as well as the three-dimensional architectures under development) has been proposed by Lange (2003), in which an overlayer of composition *equivalent to layer 1* is applied to the surface normal to the layer boundaries (see Fig. 4). The underlying assumption of this paper is that the overlayer is applied at temperature, so that the entire structure is initially stress-free and undergoes a differential contraction along with layers 1 and 2 as the structure is cooled. The purpose of this paper is to extend the work of Ho et al. (1995) to determine the stress field in the composite and to predict the effectiveness of this method for reducing and/or eliminating

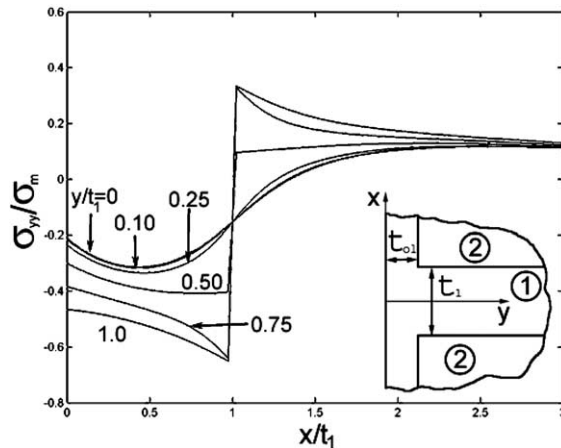


Fig. 4. Finite element results for stress field near surface with  $t_{o1} = t_1$ .

the propensity for edge cracking in a layered composite. With the stress field in hand, a numerical procedure based on superposition may be used to determine the stress intensity factor (and thus the likelihood for propagation) for incipient edge cracks at the surface of such a structure.

## 2. Stress analysis

To examine the effectiveness of overlayers, the finite element method (FEM) was employed. We continue to work under the assumption that the compressive layer is thin compared with its surrounding layers, so the stress state in the thin layer is similar to the stress state that would exist if the surrounding layers were semi-infinite in the plus and minus  $y$ -directions (see Fig. 5). In other words, we ignore the effect of the next compressive layer in the stacking sequence. A model was generated with a thickness ratio ( $t_2/t_1$ ) of 20 and a width (along the  $x$ -direction) of  $10t_1$  (Fig. 5). The composite structure consisted of one rectangular slab joined at the top to a thin interlayer and at the left boundary with an overlayer of varying thickness. The mesh consisted of four-noded, plane strain elements and was refined near the interlayer/surface juncture, where stress variation is expected to be at its highest. Initially, an elastically homogeneous case was investigated ( $E_1 = E_2$  and  $\nu_1 = \nu_2$ ). Values used in the analysis were as follows:  $E = 300$  GPa,  $\nu = 0.25$ ,  $\alpha_1 = 5.3 \times 10^{-6} \text{ C}^{-1}$ , and  $\alpha_2 = 8.3 \times 10^{-6} \text{ C}^{-1}$ . The only “loading” on the structure was through a uniform temperature change, with the difference between fabricated and cooled temperature prescribed to be  $1200 \text{ }^\circ\text{C}$ . These values were chosen to be representative of structures fabricated from alumina and alumina/mullite mixtures under development by Rao et al. (1999), Fair (2003), and Snyder (2004). However, the manner in which the results are normalized renders these actual values immaterial. The symmetry of the structure about the  $x$ -axis was utilized to reduce the mesh size, and the resulting model, with constraints, is depicted in Fig. 5. The accuracy of this model was verified by performing an analysis of the situation where the thickness of the overlayer  $t_{o1}$  was zero and comparing the FEM results to those given by the analytical

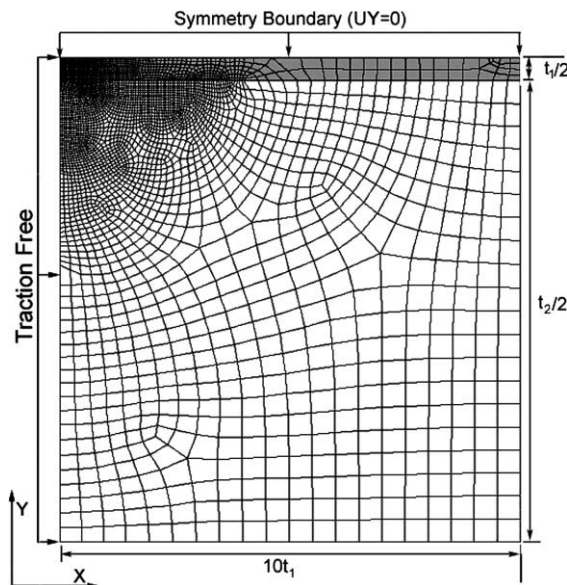


Fig. 5. Schematic of finite element model and mesh used for analysis. All nodes on top are constrained from translation in the  $y$ -direction, and all nodes on the right are constrained from translation in the  $x$ -direction (essentially, symmetry conditions). The surfaces on the left and bottom are traction-free.

solution represented by Eq. (3). From this comparison it was found that accurate results were obtained using this model, with the FEM results showing, for example, a maximum  $\sigma_{yy}$  with a  $\sim 4\%$  difference from that given by the analytical solution. Another baseline for comparison is the finite element work done by Kirchner et al. (1987). Our results for the case of no overlayer are in good agreement with results of that work. With reasonable accuracy verified, analysis of several models with  $t_{o1}$  varying between  $0.10t_1$  and  $3.00t_1$  were performed. An example of the stress results obtained are shown in Fig. 4, where  $t_{o1} = t_1$ . A more focused discussion of the results is presented in the next section.

In addition, a few cases involving elastic mismatch were examined. Models were considered with  $E_1/E_2$  ranging from 0.95 to 0.50, but with Poisson's ratio  $\nu$  maintained at 0.25. This is approximately the range that could be expected in a layered structure of alumina ( $E_2 = 401$  GPa) and an alumina/mullite mixture ( $220 \text{ GPa} < E_1 < 401 \text{ GPa}$ ). We have deferred the case of  $E_1/E_2 > 1$  to future work.

### 3. Results and discussion

A persistent result, from all cases considered, was that the maximum surface tensile stress always occurred on the centerline of layer 1. A plot of  $\sigma_{yy}$  along this centerline for various values of  $t_{o1}$  is shown in Fig. 6. We note that the case of no overlayer ( $t_{o1} = 0$ ) is identical to the result shown in Fig. 3 for  $y = 0$ . In Fig. 6, for cases with little (or no) overlayer, the surface tensile stress peaks at the surface, at or somewhat less than  $\sigma_m$ , decreases into the interior of the film and begins a relatively fast decay towards its expected far-field value of zero. As the overlayer thickens ( $t_{o1} \rightarrow t_1$ ), the magnitude of the surface stress decreases towards zero and even becomes compressive. On the other hand, the decay towards a far-field value is not as fast as with a relatively thin overlayer. Perhaps most importantly, Fig. 6 reveals that an overlayer thickness of approximately  $t_1/2$  reduces the maximum surface tensile stress to less than  $0.10\sigma_m$ .

When we plot the maximum tensile stress on the surface as a function of overlayer thickness, we observe that there is a critical value of  $t_{o1}$  for which the surface tensile stresses vanishes (Fig. 7). For this example, with no elastic mismatch, this critical value is about  $0.6t_1$ . Thus, a good design rule for such a composite fabrication technique would be to incorporate an overlayer of at least this thickness.

We do not dwell on the case of  $E_1 \neq E_2$ , since the mismatch seems to give rise to a second-order effect at best. Solutions for a range of elastic mismatches are plotted together in Fig. 8. From the interpolated curves

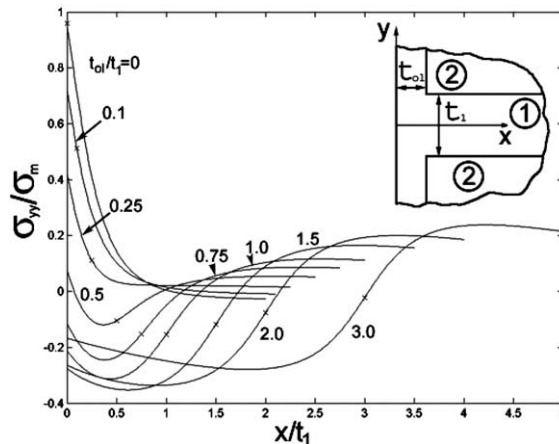


Fig. 6. Distribution of  $\sigma_{yy}$  along the centerline for various values of  $t_{o1}/t_1$ . The magnitude of the surface tensile stress decreases, and even becomes compressive, as the thickness of the overlayer increases.

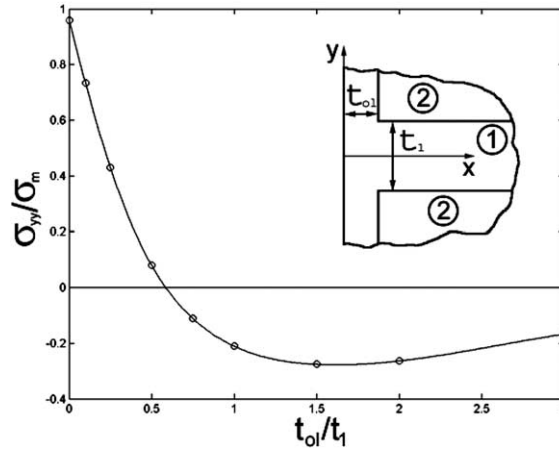


Fig. 7. Variation of  $\sigma_{yy}$  at the intersection of the centerline and surface with  $t_{o1}$ .

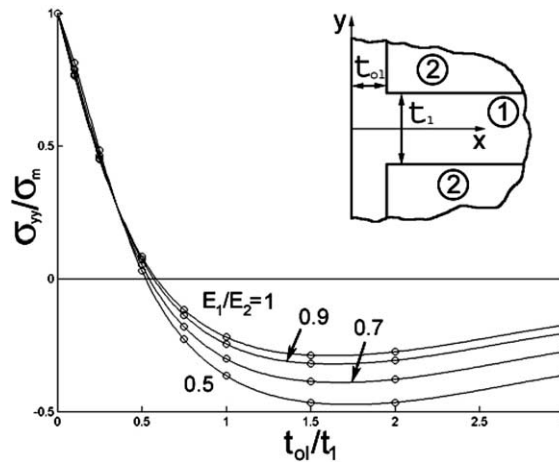


Fig. 8. Variation of  $\sigma_{yy}$  at the intersection of the centerline and surface with  $t_{o1}$  for various values of  $E_1/E_2$ .

it can be seen that, for all elastic mismatches we considered, a critical  $t_{o1}$  exists between a  $0.5t_1$  and  $0.6t_1$ , with the largest elastic mismatch having the lowest critical value of  $t_{o1}$ .

#### 4. Implications for crack extension

Suppose an edge crack is introduced into structure and propagates along the  $x$ -axis (i.e., on the centerline of the thin film). Again, we limit our consideration to plane strain, wherein the crack front is relatively long along the  $z$ -axis and the crack plane remains perpendicular to the  $y$ -axis. Moreover, we consider the so-called “edging” mode as described by Ho et al. (1995), where the crack is envisioned to propagate along the  $x$ -axis. This is to be distinguished from a “channeling” mode, where a pre-existing edge crack propagates along the  $z$ -direction. The fact that there is residual stress in the structure implies that some mode I

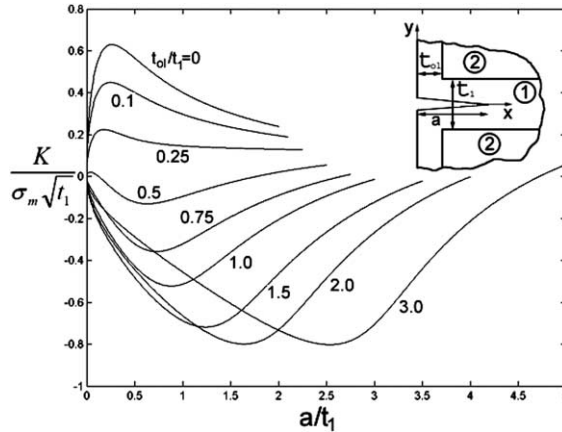


Fig. 9. Plot of stress intensity factor  $K_I$  versus crack length for various values of  $t_{01}/t_1$ .

stress intensity factor will be induced at the crack tip.<sup>2</sup> In cases where the residual field is predominantly compressive, we would expect a negative  $K_I$ , and, conversely, where the residual field is predominantly tensile, we would expect a positive value of  $K_I$ . A negative  $K_I$ , in the absence of any other sources of loading (such as a remotely applied stress), would be unphysical in the sense that the deformation would just tend to cause the crack to close against itself, as if it were not present at all. A positive value of  $K_I$  would be indicative of a driving force for crack extension, in accordance with linear elastic fracture mechanics theory. The stress intensity would depend on other variables in the problem, such as the interior layer thickness, the overlayer thickness, the magnitude of the residual stress  $\sigma_m$ , and the length of the crack.

The stress intensity factor for a crack of prescribed length  $a$  can be determined through a superposition procedure outlined by Anderson (1995), and is given by

$$K_I = \int_0^a \frac{2\sigma_{yy}(\lambda)F(\lambda/a) d\lambda}{\sqrt{\pi a}\sqrt{1 - (\lambda/a)^2}} \quad (4)$$

where  $\sigma_{yy}$  is the stress along the mid-plane in the *uncracked* solid, as calculated from the FEM method and discussed in the previous section. The “kernel” in Eq. (4), that is, every term in the integrand except  $\sigma_{yy}$ , is the stress intensity factor induced by a pair of collinear line loads of unit magnitude applied to the faces of an edge crack, at distance  $\lambda$  from the free surface, that tend to open it (Tada et al., 2000), and  $F(\xi) \approx 1.3 - 0.3\xi^{5/4}$ . After some algebraic manipulation, Eq. (4) is rendered more amenable to numerical integration, giving

$$K_I = \sigma_{yy}(a)\sqrt{\pi a} + \frac{2}{\sqrt{\pi a}} \int_0^a \frac{[\sigma_{yy}(\lambda)F(\lambda/a) - \sigma_{yy}(a)] d\lambda}{\sqrt{1 - (\lambda/a)^2}} \quad (5)$$

The results are shown in Fig. 9, as a normalized stress intensity factor against normalized crack length. For the limiting case of no overlayer, an expression for  $K_I$  is given by Tada et al. (2000). The mechanics of edge crack propagation in this limiting case were discussed in extensive detail by Ho et al. (1995), albeit in terms of the energy release rate rather than the stress intensity factor. The formalisms are completely equivalent.

<sup>2</sup> The symmetry of the problem dictates that other modes of loading are unimportant, that is,  $K_{II}$  and  $K_{III}$  vanish.

For overlayers less than about  $t_1/2$ , we note that  $K_I$  increases with crack size, i.e., the driving force increases as the crack grows. Assuming the resistance to fracture remains constant, as is typical of brittle materials, this implies that unstable crack growth would occur if any fracture process were initiated. On the other hand, for overlayer thickness greater than about  $t_1/2$ , the driving force *decreases* with increasing crack size. Stable crack growth and subsequent crack arrest would occur, if any growth occurred at all.

As pointed out earlier, the stress intensity factors calculated here are only due to the self-stress in the solid. Another contribution to the stress intensity factor could arise from external loadings (e.g., the well-known stress intensity factor of  $1.12\sigma\sqrt{\pi a}$ , due to a remotely applied tension  $\sigma$  perpendicular to the crack plane), which would superpose linearly with that given in Eq. (5). Thus, a threshold stress could be calculated using the framework outlined by Rao et al. (1999).

## 5. Summary

Finite element analysis has shown that surface tensile stresses can be reduced with the application of an overlayer. Further it has shown there is a critical thickness of  $t_{o1} = 0.6t_1$  at which this over-layer can reduce the surface tensile stresses to zero. Analysis of structures with an elastic mismatch yielded similar results, with a critical value of  $t_{o1}$  ranging between  $0.5t_1$  and  $0.6t_1$ . An analysis of the driving force on an incipient edge crack yielded similar conclusions.

## Acknowledgment

We would like to thank Fred Lange, Mark Snyder, Thomas Kiefer, Kelly da Silva, and Leah Ow for their constructive inputs. In addition, we are grateful to Haksung Moon for permission to reproduce the image in Fig. 1.

## References

- Anderson, T.L., 1995. *Fracture Mechanics: Fundamentals and Applications*, second ed. CRC Press, Ann Arbor.
- Fair, G., 2003. Processing and properties of ceramic composites with three-dimensional architectures of thin compressive layers. Ph.D. thesis, Department of Materials Science, University of California, Santa Barbara.
- Green, D.J., 1998. *Introduction to the Mechanical Properties of Ceramics*. Cambridge University Press, Cambridge.
- Hbaieb, K., McMeeking, R.M., 2002. Threshold strength predictions for laminar ceramics with cracks that grow straight. *Mechanics of Materials* 34, 755–772.
- Hillman, C., Suo, Z., Lange, F.F., 1996. Cracking of laminates subjected to biaxial tensile stresses. *Journal of the American Ceramic Society* 79 (8), 2127–2133.
- Ho, S., Hillman, C., Lange, F.F., Suo, Z., 1995. Surface cracking in layers under biaxial, residual compressive stress. *Journal of the American Ceramic Society* 78 (9), 2353–2359.
- Jónsdóttir, F., Beltz, G.E., McMeeking, R.M. Modeling of threshold strength in 3D ceramic structures. *Journal of Applied Mechanics*, in press.
- Kirchner, H.P., Conway Jr., J.C., Segall, A.E., 1987. Effect of joint thickness and residual stresses on the properties of ceramic adhesive joints: I. Finite element analysis of stresses in joints. *Journal of the American Ceramic Society* 70 (2), 104–109.
- Lange, F.F., 1989. Powder processing science and technology for increased reliability. *Journal of the American Ceramic Society* 72 (1), 3–15.
- Lange, F.F., 2003. private communication.
- Lawn, B., 1993. *Fracture of Brittle Solids*, second ed. Cambridge University Press, Cambridge.
- McMeeking, R.M., Hbaieb, K., 1999. Optimal threshold strength of laminar ceramics. *Zeitschrift für Metallkunde* 90 (12), 1031–1036.
- Oechsner, M., Hillman, C., Lange, F.F., 1996. Crack bifurcation in laminar ceramic composites. *Journal of the American Ceramic Society* 79 (7), 1834–1838.

- Rao, M.P., Sánchez-Herencia, A.J., Beltz, G.E., McMeeking, R.M., Lange, F.F., 1999. Laminar ceramics that exhibit a threshold strength. *Science* 286, 102–105.
- Snyder, M., 2004. Ceramic composites with pseudo-three dimensional architectures designed to produce a threshold strength. Ph.D. Thesis, Department of Materials Science, University of California, Santa Barbara.
- Tada, H., Paris, P.C., Irwin, G.R., 2000. *The Stress Analysis of Cracks Handbook*, third ed. American Society of Mechanical Engineers, New York.